[19]J. S. Jayson, R. N. Bhargava, and R. W. Dixon, J. Appl. Phys. 41, 4972 (1970).

[20]See, for example, the review article by V. L. Bonch-Bruevich and E. G. Landsberg, Phys. Status Solidi 29, 9 (1968).

[21]P. T. Landsberg, C. Phys-Roberts, and P. Lal, Proc. Phys. Soc. (London) 84, 915 (1964).

[22]J. D. Cuthbert, C. H. Henry, and P. J. Dean, Phys. Rev. 170, 739 (1968).

[23]E. I. Tolpygo, K. B. Tolpygo, and M. K. Sheinkman, Fiz. Tverd. Tela 7, 1790 (1965) [Soviet Phys. Solid State 7, 1442 (1965)].

[24]Below $\sim 60\,°K$ minority carriers are generated by means of a two-step process involving the oxygen donor [J. M. Dishman (unpublished)]. This is a second-order process, however, in comparison to the Auger processes discussed here.

[25]A summary of several model calculations for the FB temperature dependence is found in Ref. 13. The strongest T dependence in which the transition rate decreases with temperature is for the simple hydrogenic model of Sclar and Burnstein (Ref. 26) which gives

$$B_{\text{FB}} \propto T^{-1/2}.$$

[26]N. Sclar and E. Burnstein, Phys. Rev. 98, 1757 (1955).

[27]D. M. Eagles, J. Phys. Chem. Solids 16, 76 (1960).

[28]W. P. Dumke, Phys. Rev. 132, 1998 (1963).

[29]L. Bess, Phys. Rev. 105, 1469 (1957).

[30]L. R. Weisberg, J. Appl. Phys. 39, 6096 (1968).

[31]J. M. Dishman (unpublished).

[32]G. L. Pearson and J. Bardeen, Phys. Rev. 75, 865 (1949).

[33]R. C. Enck and A. Honig, Phys. Rev. 177, 1182 (1969).

[34]V. L. Bonch-Bruevich, Zh. Eksperim. i Teor. Fiz. 32, 1092 (1957) [Soviet Phys. JETP 5, 894 (1957)].

[35]A. Miller and B. Friedman (unpublished), as quoted in Ref. 33, find that the DA recombination rate is $W(R) \propto E_A^{5/2} E_O^{3/2} e^{-2R/a_A}$, where R is the pair separation. Integrating this expression over a random distribution of pair separations yields a total rate $r_{\text{DA}} \propto E_A E_O^{3/2}$, whose E_A dependence is the same as Eq. (16).

[36]M. K. Sheinkman, Fiz. Tverd. Tela 5, 2780 (1963) [Soviet Phys. Solid State 5, 2035 (1963)].

Electroreflectance Spectra of CdSiAs₂ and CdGeAs₂

J. L. Shay

Bell Telephone Laboratories, Holmdel, New Jersey 07733

and

E. Buehler

Bell Telephone Laboratories, Murray Hill, New Jersey 07974

(Received 2 November 1970)

We report electroreflectance spectra for the chalcopyrite crystals CdSiAs₂ and CdGeAs₂. These compounds are characterized by large built-in compressions and internal displacements of the As anions due to the difference in the cation covalent radii, Cd being 27% larger than Si and 21% larger than Ge. We find that CdSiAs₂ has a direct band gap at 1.55 eV. The simple quasicubic model for the crystal field splitting of the fundamental band gap in chalcopyrite crystals breaks down in CdSiAs₂ because of a contribution ($\sim 50\%$ of the compressional splitting) of opposite sign due to the difference in the pseudopotentials of the cations Cd and Si. However, the quasicubic model quantitatively explains the observed polarization dependences in terms of the measured valence band splittings. Transitions corresponding to the Λ transitions in zinc-blende crystals are not observed in CdSiAs₂ and CdGeAs₂. Instead, a new doublet is observed for $\vec{E} \perp Z$ in both crystals, and we assign this new structure to transitions at the point N in the chalcopyrite Brillouin zone.

I. INTRODUCTION

Many of the electronic and optical properties of II-IV-V₂ chalcopyrite semiconductors can be understood in terms of a simple binary-ternary analogy which emphasizes the similarity of the zinc-blende and chalcopyrite lattices.[1-5] In previous electroreflectance studies[1-4] of CdSnP₂ and ZnSiAs₂, a simple quasicubic model accounting for the built-in compression of the chalcopyrite lattice quantitatively explained the (i) ordering, (ii) splittings, and (iii) polarization dependences for the three transitions derived from the triply degenerate fundamental band gap $\Gamma_{15} \rightarrow \Gamma_1$ in zinc-blende crystals. A quasicubic model was also constructed to explain the splittings and polarization dependences of the transitions in CdSnP₂ and ZnSiAs₂ corresponding to the Λ transitions in zinc-blende crystals. Other electroreflectance structure was attributed to pseudodirect transitions—direct transitions in chalcopyrite corresponding to indirect transitions in zinc-blende crystals which become allowed because of the doubling of the unit cell along the Z direction in chalcopyrite crystals.

Such a simple analogy is expected to break down in CdSi or CdGe compounds because of the difference in size of the cations, Cd being 27% larger than Si and 21% larger than Ge. This difference in size triggers a built-in uniaxial compression and an internal strain, a distortion of the column V anions away from the $\frac{1}{4}\frac{1}{4}\frac{1}{4}$ positions. The antisymmetric potential resulting from the difference of the cation pseudopotentials should also become important for CdSi compounds, since Cd and Si are two rows apart on the Periodic Chart. Consequently, in the present electroreflectance studies of CdSiAs₂ and CdGeAs₂, we address ourselves to the question: To what extent is CdSiAs₂ basically a slightly perturbed GaAs? To summarize our results, we find that the fundamental band gap of CdSiAs₂ is derived from the triply degenerate Γ_{15} → Γ_1 fundamental gap of GaAs, but the valence band splittings predicted for CdSiAs₂ by the simple model accounting for compression alone are no longer quantitatively accurate. The difference in Cd and Si potentials make a contribution to the crystal field splitting of the valence bands ~ 50% of the stress splitting and of opposite sign. For the higher energy gaps, the breakdown of the simple analogy is much more drastic. No electroreflectance peaks are observed in CdSiAs₂ or CdGeAs₂ corresponding to the Λ transitions in GaAs. Instead a new doublet is observed in both crystals for $\vec{E} \perp Z$ and is assigned to transitions at the point N.

II. EXPERIMENTAL TECHNIQUES

The CdSiAs₂ crystals were grown by a closed-tube chemical-transport technique using a small amount of SnCl₂ as the source of Cl₂ for the transport of Si. Although not intentionally doped, a thermal probe indicated that the crystals were p type. The CdGeAs₂ crystals were grown from the melt and also were p type. A more detailed discussion of the crystal growth is presented elsewhere.[6]

The electroreflectance measurements were performed using the electrolyte technique developed by Cardona and co-workers.[7] For both CdSiAs₂ and CdGeAs₂, reverse biasing of the semiconductor-electrolyte junction was obtained for negative voltages applied to the crystal. For $V_{dc} = -1.5\,V$, reverse currents of about 1 μa were obtained. CdSiAs₂ crystals did not show any deterioration during the course of an experiment. CdGeAs₂ crystals, however, gradually accumulated a metalliclike film in the 1-molar KCl-H₂O electrolyte. Consequently, experiments were performed on several crystals from the same boule in order to obtain reliable results over the entire wavelength range. CdSiAs₂ crystals were etched for 1 min in 1% Br₂ in methanol; CdGeAs₂ crystals

were Syton polished.[8] Soldered indium contacts made Ohmic contact to both materials. Electroreflectance studies were performed on {112} and {011} natural faces, which were identified by Laue photographs and x-ray diffraction studies.[2,3] For reflectance studies on these faces, it is possible to polarize light with the electric vector perpendicular to the optic axis, but not completely parallel to this axis. Consequently, in the electroreflectance spectra, $E \parallel Z$ is only nominal, and in fact only $\frac{2}{3}$ or $\frac{4}{5}$ of the intensity lies parallel to Z for {112} and {011} faces, respectively.

The electroreflectance spectrum associated with any given critical point can, in general, have oscillatory structure above and below the critical point. Consequently, a discussion of our procedure for determining the energy gaps from the spectra in the present work is in order. In general, we locate the critical point at the lowest-energy prominant peak of the structure. The maximum uncertainty in such an identification is the peak's width. Although this is a reliable procedure for M_0 critical points at the fundamental edge, structure associated with M_1 critical points can have, for example, two peaks of equal height in which case the energy gap is somewhere in between. For most of the electroreflectance spectra reported here, each individual structure displays only one prominant peak which we identify as the critical point at the energy gap.
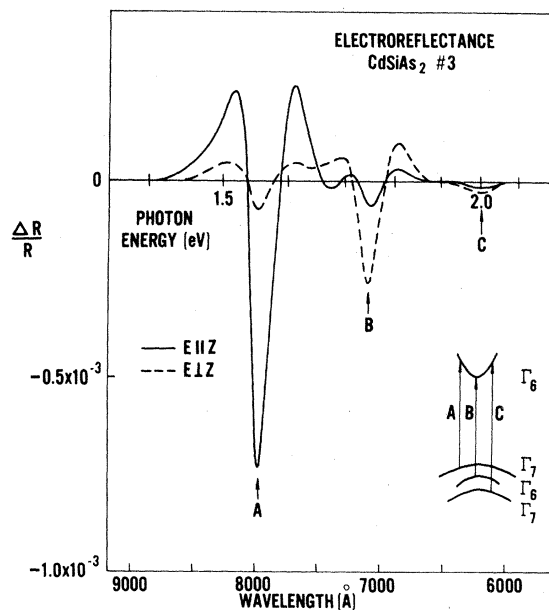

FIG. 1. Room-temperature electrolyte electroreflectance spectra of CdSiAs₂ for light polarized relative to the optic axis. The orientation was [112], so $E \parallel Z$ is only nominal and only $\frac{2}{3}$ of the intensity is parallel to Z, $V_{dc} = -1.5$ V; $V_{ac} = 1.0 V_{pp}$.
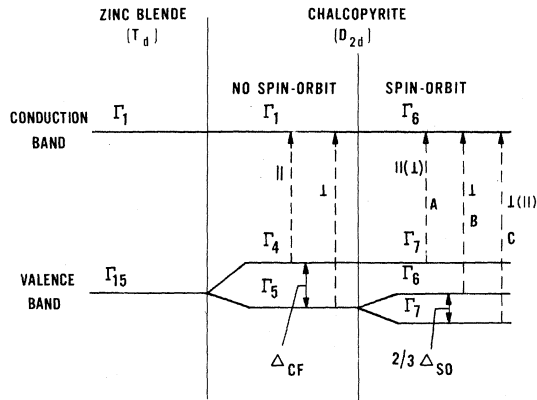
FIG. 2. Band structure and selection rules for the transitions in chalcopyrite crystals derived from the $\Gamma_{15} \to \Gamma_1$ energy gap in zinc-blende crystals. The splittings and polarization dependences are indicated schematically for a crystal in which $\Delta_{so} \ll \Delta_{cf}$. For arbitrary values of these parameters, the valence-band splittings and polarization dependences are given, respectively, by Eqs. (1) and (3) in the text.

III. EXPERIMENTAL RESULTS

A. Lowest Energy Gap

In Fig. 1, we present the 300 °K electrolyte electroreflectance spectra for a single crystal of $CdSiAs_2$ measured, respectively, for light polarized parallel and perpendicular to the optic axis. As has been previously observed[1-4] in $CdSnP_2$ and $ZnSiAs_2$, the A, B, and C peaks at 1.55, 1.74, and 1.99 eV are derived from the $\Gamma_{15} \to \Gamma_1$ transition in zinc blende according to the model shown in Fig. 2. The triple degeneracy of the Γ_{15} valence band is completely lifted in chalcopyrite under the simultaneous perturbations of spin-orbit coupling and the noncubic crystalline field. The group theoretical selection rules are indicated in Fig. 2. Whereas the B peak is only allowed for $\vec{E} \perp Z$, it is partially observed in the solid curve in Fig. 1 due to the experimental constraint that $\vec{E} \parallel Z$ is

only nominal as explained earlier. The energies, polarizations, and identifications of $CdSiAs_2$ electroreflectance structure are summarized in Table I.

The ordering and splittings of the A, B, and C peaks in $CdSnP_2$ and $ZnSiAs_2$ have been explained[1-4] by a simple model which regards a chalcopyrite crystal, e.g., $CdSiAs_2$, as a strained version of its binary analog, e.g., GaAs. Within this so-called quasicubic model, the energies of the Γ_7 valence-band levels relative to the Γ_6 level are given by[9,10]

$$E_{1,2} = \tfrac{1}{2}(\Delta_{so} + \Delta_{cf}) \pm \tfrac{1}{2}[(\Delta_{so} + \Delta_{cf})^2 - \tfrac{8}{3}\Delta_{so}\Delta_{cf}]^{1/2}, \quad (1)$$

where Δ_{so} is the spin-orbit splitting measured in GaAs, the binary analog of $CdSiAs_2$, and Δ_{cf} is the crystal-field-splitting parameter. Considering only the effects of the built-in compression of the chalcopyrite lattice, we estimate Δ_{cf} by

$$\Delta_{cf} = \tfrac{3}{2}b(2 - C/A), \quad (2)$$

where b is the deformation potential describing the splitting of the valence bands in the zinc-blende binary analog under uniaxial stress,[11,12] and C and A are the chalcopyrite lattice constants.[13] The experimental parameters Δ_{so} and Δ_{cf}, determined from the splitting of the A, B, and C peaks using Eq. (1), are summarized in Table II together with the theoretical values predicted by the quasicubic model. The agreement between theory and experiment is not as good for $CdSiAs_2$ as it is for the other two crystals, especially for Δ_{cf} the crystal field splitting. This breakdown of the simple theory in $CdSiAs_2$ will be discussed in a later Sec. IV A.

In addition to the eigenvalues given by Eq. (1), the quasicubic model determines eigenfunctions from which one can predict polarization dependences.[1-4] For this model, the ratio of the strengths of transitions from a given Γ_7 valence band to the Γ_6 conduction band for light polarized, respectively, parallel or perpendicular to the optic axis is given by[9]

TABLE I. $CdSiAs_2$ electroreflectance structure.

Label	Energy (eV)	Polarization	Identification	Zinc-blende analog
A	1.55	$\parallel$	$\Gamma_7 \to \Gamma_6$	E_0,
B	1.74	$\perp$	$\Gamma_6 \to \Gamma_6$	$E_0 + \Delta_0$
C	1.99	$\perp, \parallel$	$\Gamma_7 \to \Gamma_6$	
P_3	{2.50 / 2.57}	$\parallel$ / $\perp$	$N_1 \to L_1$	
D	{2.99 / 3.10}	$\perp$ / $\perp$	$N_1 \to N_1$ / $N_1 \to N_1$	$L_3 \to L_1$
P_2	3.82	$\perp$	$X_5 \to \Gamma_1$	
	3.97	$\perp, \parallel$		
	4.23	$\parallel$		

TABLE II. Comparison of experimental results and theoretical predictions of the quasicubic model for the valence-band structure of $CdSnP_2$, $ZnSiAs_2$, and $CdSiAs_2$.

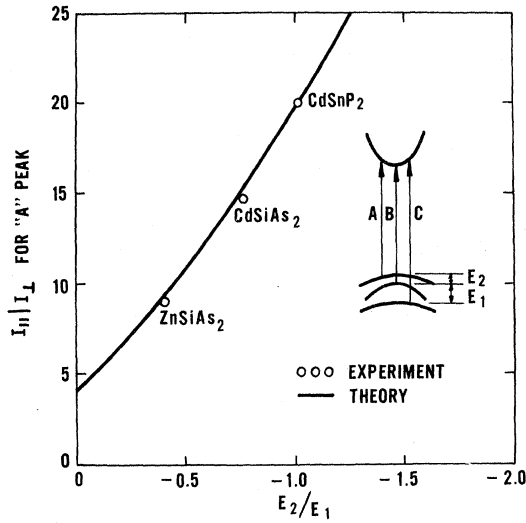|		Δ_{so} (eV)	Δ_{cf} (eV)	$I_\parallel / I_\perp$ A	B	C
$CdSnP_2$	Experiment[a]	0.10	-0.10	≥ 20	~ 0.2	~ 0.1
	Theory	0.11	-0.12	20	0	0.3
$ZnSiAs_2$	Experiment[b]	0.28	-0.13	9	~ 0	~ 0.5
	Theory	0.31	-0.16	8.5	0	0.5
$CdSiAs_2$	Experiment	0.29	-0.24	15	~ 0	~ 0.2
	Theory	0.34	-0.43	16	0	0.2

[a]See Ref. 2.　　　　　　　[b]See Ref. 3.

FIG. 3. Comparison of experimental and theoretical [Eq. (3)] polarization intensity ratios for the *A* transition.

$$I_\parallel / I_\perp = (2 - 3E/\Delta_{so})^2 . \qquad (3)$$

Using experimental values for E and Δ_{so}, the predictions of Eq. (3) are given in Table II together with the experimental intensity ratios. The intensity ratio predicted by Eq. (3) is also shown as the solid line in Fig. 3 where the points are experimental data. It is apparent that the quasicubic model quantitatively explains the observed polarization dependences.

B. Higher Energy Gaps
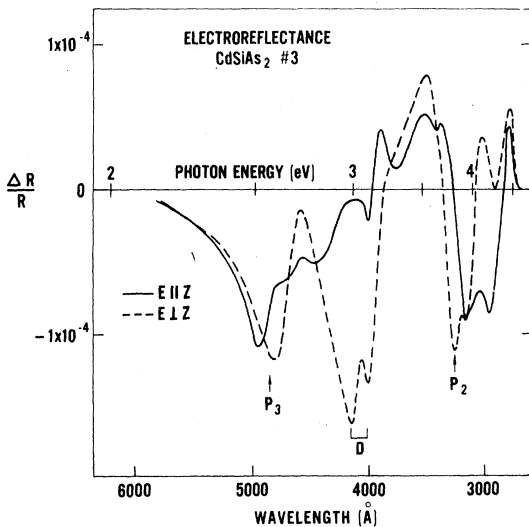
The electroreflectance spectra for CdSiAs₂ and

FIG. 4. Room-temperature electrolyte electroreflectance spectra of CdSiAs₂ in the 2.0–4.5-eV region; the orientation is [112], $V_{dc} = -1.5$ V; $V_{ac} = 1.0 V_{pp}$.
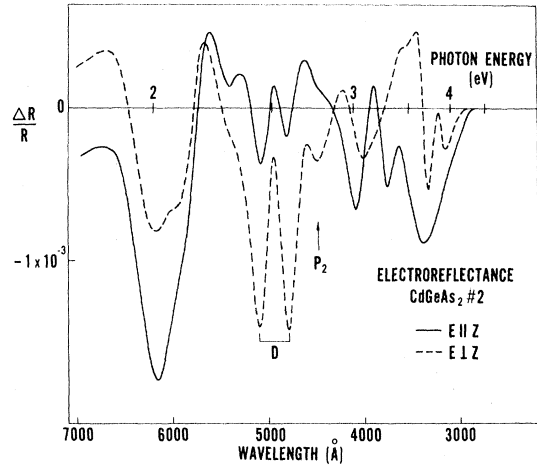

FIG. 5. Room-temperature electrolyte electroreflectance spectra of CdGeAs₂ in the 2.0- to 4.5-eV region. The orientation is nearly [011], $V_{dc} = -1.5$ V; $V_{ac} = 10 V_{pp}$.

CdGeAs₂ in the energy range 2–4.5 eV are shown in Figs. 4 and 5, respectively. The *A*, *B*, and *C* peaks were not observed in CdGeAs₂, since they lie below the infrared cutoff of the electrolyte. The general features of the data in Fig. 5 agree with the unpolarized data of Kwan and Woolley[14] obtained on polycrystalline samples.

The spectra in Figs. 4 and 5 are quite different from previous results for CdSnP₂[2] and ZnSiAs₂[3] in which one could identify doublets derived from the E_1 and $E_1 + \Delta_1$ peaks in zinc blende. The measured splittings were approximately equal to $\frac{2}{3}\Delta_{so}$ as expected. Strong supporting evidence for the identifications in both crystals were the observed polarization properties: E_1 was stronger for $E \parallel Z$, whereas $E_1 + \Delta_1$ was stronger for $E \perp Z$, and the intensity ratios were in reasonable agreement with a simple theory.[3] For CdSiAs₂ and CdGeAs₂, the E_1 peaks should lie between 2.5 and 3.0 eV, be split ~ 0.2 eV, and display intensity ratios of about 2 and 0.6 for the E_1 and $E_1 + \Delta_1$ peaks, respectively. No such doublet can be found in either Fig. 4 or 5. Instead, the striking feature of the spectra in this energy range is a doublet, labeled D, with both peaks strongly polarized $E \perp Z$. In Sec. IV, we show that D is probably due to transitions at the point N in the chalcopyrite Brillouin zone.

IV. DISCUSSION

A. Lowest Energy Gap

The binary-ternary analogy which has been used to explain[1-4] many of the electronic properties of CdSnP₂ and ZnSiAs₂ is shown schematically in Fig. 6. One assumes that the crystal potential in a chalcopyrite crystal, e.g., CdSiAs₂, is

BINARY - TERNARY ANALOGY

CdSiAs$_2$ $\simeq$ 2[GaAs]

  + COMPRESSION

  + DOUBLE UNIT CELL

  + ANTISYMMETRIC POTENTIAL

  + INTERNAL STRAIN

FIG. 6. Binary-ternary analogy for relating electronic and optical properties of ternary chalcopyrite crystals to properties of the well-understood binary zinc-blende crystals.

approximately the same as the crystal potential in the zinc-blende binary analog, e.g., GaAs, except for four perturbations: (i) The chalcopyrite lattice has a built-in uniaxial compression along the Z axis; (ii) the ordering of the cations relative to one another is such that the unit cell is doubled along the Z axis; (iii) the difference in the pseudopotentials of the cations (e.g., Cd and Si) produces a new antisymmetric potential; and (iv) there is an internal strain, i.e., the anions are not located at $\frac{1}{4}\frac{1}{4}\frac{1}{4}$, etc., but are slightly distorted in such a way as to reduce the IV-V bond lengths.

As shown in Sec. III and summarized in Table II, the effects of compression alone explain the structure of the valence band maxima in CdSnP$_2$ and ZnSiAs$_2$ but are in error by a factor of ~2 in CdSiAs$_2$. Due to the great difference in the covalent radii of Cd and Si,[15] the crystal lattice of CdSiAs$_2$ displays a large built-in compression and a large internal strain. The antisymmetric potential due to the difference in cations should also become important in CdSiAs$_2$ since Cd and Si are two rows apart on the Periodic Chart. The built-in compression and the antisymmetric potential have been explicitly included in a recent pseudopotential calculation by Goryunova et al.,[16] whose results are included in Table III. The good agreement between the pseudopotential predictions and experiment as shown in Table III apparently indicates that the large internal strain in CdSiAs$_2$ is of relatively little importance in determining the splitting of the valence-band maxima. The difference between the simple theory of Eq. (2) and experiment is therefore entirely due to the antisymmetric potential resulting from the differences in the Cd and Si pseudopotentials, even though this antisymmetric potential contributes to Δ_{cf}

FIG. 7. Lowest-order approximation to the energy-band structure of CdSiAs$_2$ (solid lines) obtained by imbedding the energy bands of GaAs (dashed lines) (Ref. 19) into the chalcopyrite Brillouin zone.

only in second order.[17]

B. Higher Energy Gaps

Extending the binary-ternary analogy of Fig. 6 to the higher energy gaps, one can account for the doubling of the unit cell in CdSiAs$_2$ along the Z direction by merely imbedding the energy bands of GaAs into the chalcopyrite Brillouin zone.[17,18] The results of this procedure are shown in Fig. 7 where the dashed curves are the energy bands of GaAs calculated by Cohen and Bergstresser,[19] and the solid lines are the energy bands of CdSiAs$_2$ in this approximation. Two types of energy gaps result: (a) direct energy gaps corresponding to direct gaps in GaAs; and (b) pseudodirect energy gaps, which are direct energy gaps corresponding to indirect gaps in GaAs. We have referred to the latter as pseudodirect[2,3] since their strengths depend upon the degree of difference of the cation pseudopotentials. Of the four pseudodirect transitions P_1–P_4 indicated in Fig. 7, only two, P_2 and P_3, are observed in CdSiAs$_2$ (Fig. 4). The experimental energies of peaks P_2 and P_3 are close to the transition energies in Fig. 7 and their polarization properties are as expected.[2,3] P_2 is also tentatively identified in Fig. 5.

For both CdSnP$_2$[2] and ZnSiAs$_2$[3] a quasicubic model has also been constructed to explain the effects of the built-in compression upon the Λ transitions. As discussed earlier, although the simple theory explained the splitting and polarization dependences of these transitions in CdSnP$_2$

TABLE III. Comparison of theoretical and experimental values for Δ_{cf}, the crystal field splitting of the valence-band maxima (in eV).

	CdSnP$_2$	ZnSiAs$_2$	CdSiAs$_2$
Experiment	−0.10[a]	−0.13[b]	−0.24
Theory [Eq. (2)]	−0.12	−0.16	−0.43
Theory (pseudopotential[c])	−0.14	−0.20	−0.29

  ^{a}See Ref. 2. ^{b}See Ref. 3. ^{c}See Ref. 16.

and $ZnSiAs_2$, no Λ transitions are apparent in the electroreflectance spectra of $CdSiAs_2$ (Fig. 4) or $CdGeAs_2$ (Fig. 5). Instead of a doublet D, strongly polarized $E \perp Z$ is observed in this energy range in both crystals. This breakdown of the simple theory for the Λ transitions is not surprising in view of our earlier discussion of the breakdown of the simple theory for the valence-band structure in $CdSiAs_2$.

The L point in zinc-blende maps to N in chalcopyrite on account of the doubling of the unit cell along the Z direction. In view of the similarity of the D splittings to the spin-orbit splitting of L_3 in GaAs, and the closeness of the D energies to the $L_3 \rightarrow L_1$ energy gap in GaAs, it appears likely that the D doublet is due to $N_1 \rightarrow N_1$ transitions, derived from $L_3 \rightarrow L_1$ transitions in zinc blende. Until a theoretical calculation unravels the valence-band structure at N, this assignment cannot be unambiguously confirmed.

V. CONCLUSIONS

The fundamental band gap of $CdSiAs_2$ is derived from the $\Gamma_{15} \rightarrow \Gamma_1$ transition in GaAs, but the triple degeneracy of the Γ_{15} valence band is completely removed by the combined effects of spin-orbit interaction and the noncubic crystalline field. The observed crystal field splitting results from a partial cancellation of a large contribution $(-0.43\,eV)$ due to the built-in uniaxial compression, and a contribution of opposite sign $(+0.19$

eV) due to the large differences in the Cd and Si pseudopotentials. Using the experimental splittings of the valence bands, the quasicubic model quantitatively explains the amplitudes of the observed polarization dependences.

The electroreflectance structure corresponding to higher energy gaps in $CdSiAs_2$ and $CdGeAs_2$ are quite different from previous studies of $CdSnP_2$[2] and $ZnSiAs_2$.[3] This result is not unexpected in view of the breakdown of the simple compressional model for the structure of the valence-band maxima in $CdSiAs_2$. In both $CdSiAs_2$ and $CdGeAs_2$, no electroreflectance structure is observed corresponding to the Λ transitions in GaAs. Instead, a doublet labeled D is observed in both crystals for $\vec{E} \perp Z$ near the expected energies of the Λ transitions. We attribute D to $N_1 \rightarrow N_1$ transitions derived from the $L_3 \rightarrow L_1$ energy gap in GaAs.

[1]J. L. Shay, E. Buehler, and J. H. Wernick, Phys. Rev. Letters **24**, 1301 (1970).

[2]J. L. Shay, E. Buehler, and J. H. Wernick, Phys. Rev. B **2**, 4104 (1970); *Proceedings of the Tenth International Conference on the Physics of Semiconductors*, edited by S. P. Keller, J. C. Hensel, and F. Stern (USAEC, 1970), p. 589.

[3]J. L. Shay, E. Buehler, and J. H. Wernick, Phys. Rev. B **3**, 2004 (1971).

[4]J. E. Rowe and J. L. Shay, Phys. Rev. B **3**, 451 (1971).

[5]For a recent review, see N. A. Goryunova, *International Conference on the Physics of Semiconductors, Moscow*, 1968 (Publishing House Nauka, Leningrad, 1968), p. 1198.

[6]E. Buehler and J. H. Wernick, J. Crystal Growth (to be published).

[7]M. Cardona, K. L. Shaklee, and F. H. Pollak, Phys. Rev. **154**, 696 (1967); M. Cardona, *Solid State Physics* (Academic, New York, 1969), Suppl. 11.

[8]Syton HT; Monsanto Chemical Co., 277 Park Avenue, New York, N. Y. 10017.

[9]J. J. Hopfield, J. Phys. Chem. Solids **15**, 97 (1960). Our sign convention for Eqs. (1) and (3) is in agreement with this reference.

[10]Our symmetry notation is taken from G. F. Koster, J. O. Dimmock, R. G. Wheeler, and H. Statz, *Properties of the Thirty-Two Point Groups* (MIT Press,

Cambridge, 1963). A single exception is the zinc-blende level Γ_{15} which we identify with Γ_5 in the point group T_d. In the Russian literature, a quite different notation is used for the extra representations of the chalcopyrite point group D_{2d}.

[11]F. H. Pollak and M. Cardona, Phys. Rev. **172**, 816 (1968).

[12]A. Gavini and M. Cardona, Phys. Rev. B **1**, 672 (1970).

[13]A. S. Borshchevskii, N. A. Goryunova, F. T. Kesamanly, and D. N. Nasledov, Phys. Status Solidi **21**, 9 (1967).

[14]C. C. Y. Kwan and J. C. Woolley, Can. J. Phys. **48**, 2085 (1970).

[15]We estimate the bond lengths in the ternaries using L. Pauling's covalent radii, in *The Nature of the Chemical Bond* (Cornell U. P., Ithaca, N. Y., 1960), p. 246; S. Abrahams and J. Bernstein, J. Chem. Phys. **52**, 5607 (1970), have shown that for $ZnSiP_2$, $CdGeP_2$, and $CdGeAs_2$ the measured bond lengths are very close to the values predicted using Pauling's covalent radii.

[16]N. A. Goryunova, A. S. Poplavnoi, Yu. I. Polygalov, and V. A. Chaldyshev, Phys. Status Solidi **39**, 9 (1970).

[17]G. F. Karavaev and A. S. Poplavnoi, Fiz. Tverd. Tela **8**, 2143 (1966) [Sov. Phys. Solid State **8**, 1704 (1967)]; G. F. Karavaev, A. S. Poplavnoi, and V. A. Chaldyshev, Fiz. Tekh. Poluprov. **2**, 113 (1968) [Sov. Phys. Semiconductors **2**, 93 (1968)].

[18]V. A. Chaldyshev and V. N. Pokrovskii, Izv. Vuz. USSR Fiz. 2, 173 (1960); 5, 103 (1963).

[19]M. L. Cohen and T. K. Bergstresser, Phys. Rev. 141, 789 (1966).

Optical Absorption Spectrum of AgF

Alfred P. Marchetti and G. L. Bottger

Research Laboratories, Eastman Kodak Company, Rochester, New York 14650

(Received 9 December 1970)

The optical absorption of thin films of silver monofluoride has been investigated in the visible and ultraviolet region of the spectrum at room and low temperatures. Exciton peaks have been observed at 4.63 and 6.34 eV for samples at 4.8 °K. The first exciton peak is considerably lower in energy than might be expected on the basis of the trend set by the other silver halides. This unusually low energy has led us to speculate that the band structure of AgF may be quite different from those of the other silver halides.

I. INTRODUCTION

Although the optical absorption spectra of the common silver halide crystals (i.e., AgCl, AgBr, and AgI) have been studied extensively,[1] no information has been reported on the absorption spectrum of silver monofluoride crystals. This omission is related to various untoward properties of silver monofluoride which cause its preparation in a pure state to be difficult. Like the other silver halides it is sensitive to light, but unlike the other silver halides it is hygroscopic and highly reactive, and decomposes on melting. Moreover, three different fluorides of silver are known to exist[2]—silver monofluoride (AgF), silver subfluoride (Ag_2F), and silver difluoride (AgF_2).

One of the few published studies on AgF was of its gas-phase absorption spectrum, in which the 0, 0 energy and vibrational constants of the $^3\Pi_0^*$ ←$^1\Sigma$ transition were determined.[3] These constants were compared with those of AgCl, AgBr, and AgI, and were found to be in accord with the trends set by the other three members of the series. In the gas phase, however, the silver halides are expected to act as diatomic molecules; thus, this study provides little insight into the optical properties of AgF crystals.

The present study of the visible and ultraviolet absorption spectrum of AgF was undertaken on thin films. The observed optical spectrum of AgF differs significantly from predictions based on simple considerations of the spectra of the other silver halides. We discuss the unusual behavior found in terms of the theoretical framework available at present.

II. EXPERIMENTAL

Thin films of AgF were prepared from commer-

cially available silver monofluoride using a fractional evaporation technique in vacuum under red light. The silver monofluoride starting materials obtained from a number of sources varied in color from yellow to black, and were always contaminated with silver, silver oxide, water, and various trace impurities. A particular sample of chemically pure grade AgF, purchased from the Amend Drug and Chemical Co., Inc., was found to be relatively pure and was used in these studies. Analysis of this commercial sample by flame emission spectroscopy, together with spark-source mass spectroscopy, showed the major trace impurities listed in Table I. In one case where the AgF had contacted glass, additional impurities of silicon, calcium, and the alkali metals were found. The films were formed by evaporating the dried commercial AgF sample from a pyrolitic graphite boat at a rate of approximately 0.05 μ/h. At faster deposition rates, large amounts of colloidal silver were often formed in the evaporated layers. The film thickness was measured by a Sloan thickness monitor[4] and by x-ray fluorescence studies of the silver in the film.

The AgF films were deposited on single-crystal CaF_2 substrates which were held at about 80 °C during evaporation. Analysis of the films by spark-source mass spectroscopy indicated that they generally contained a level of trace impurities similar to that found in the commercial AgF starting material. Visual examination of the films showed them to be colorless, presumably indicating that the concentration of colloidal silver and other colored impurities was substantially reduced. An investigation of the layers by x-ray diffraction showed them all to be crystalline and highly oriented, with the (111) planes parallel to the surface of the CaF_2 substrate. The orientation of the AgF film was due